JOURNAL OF THERMOPHYSICS AND HEAT TRANSFER
Vol. 22, No. 3, July–September 2008

Analytical Modeling of Fluid Flow and Heat Transfer in Microchannel/Nanochannel Heat Sinks

W. A. Khan*
National University of Science and Technology, PNS Jauhar, Karachi 75350, Pakistan
and
M. M. Yovanovich†
University of Waterloo, Waterloo, Ontario N2L 3G1, Canada

DOI: 10.2514/1.35621

Laminar forced convection in two-dimensional rectangular microchannels and nanochannels under hydrodynamically and thermally fully developed conditions is investigated analytically in the slip-flow regime. Closed-form solutions for fluid friction and Nusselt numbers are obtained by solving the continuum momentum and energy equations with the first-order velocity slip and temperature jump boundary conditions at the channel walls. An isoflux thermal boundary condition is applied on the heat sink base. The results of the present analysis are presented in terms of the channel aspect ratio, hydraulic diameter, momentum and thermal accommodation coefficients, Knudsen number, slip velocity, Reynolds number, and Prandtl number. It is found that fluid friction decreases and heat transfer increases compared with no-slip flow conditions, depending on the aspect ratios and Knudsen numbers that include the effects of the channel size or rarefaction and the fluid/wall interaction.

Nomenclature

A = total heating surface area, m^2, or constant, $-(1/2\mu)/(\Delta P/L)$
A_c = cross-sectional area of a single fin, m^2
D_h = hydraulic diameter, m
f = skin-friction coefficient or friction factor
G = volume flow rate, cm^3/s
H_c = channel height, m
h = average heat transfer coefficient, $W/m^2 \cdot K$
K = coefficient of pressure loss, $\Delta P/\frac{1}{2}\rho U_{av}^2$
Kn = Knudsen number, λ/D_h
k = thermal conductivity of solid, $W/m \cdot K$
k_{ce} = sum of contraction and expansion losses in the channel
k_f = thermal conductivity of fluid, $W/m \cdot K$
L = length of the channel in the flow direction, m
$\mathcal{L}$ = characteristic length, usually taken as the hydraulic diameter of the channel, m
m = fin parameter, m^{-1}, $\sqrt{h_{av}/k(2w_w)}$
$\dot{m}$ = total mass flow rate, m^{-1}, kg/s
N = total number of microchannels/nanochannels
Nu_{D_h} = Nusselt number based on hydraulic diameter
Pe_{D_h} = Peclet number based on hydraulic diameter
Pr = Prandtl number
Q_b = heat transfer rate from heat sink base, W
Q_{fin} = heat transfer rate from fin, W
q = heat flux, W/m^2
Re_{D_h} = Reynolds number based on hydraulic diameter, $U_{av}D_h/\nu$
T = absolute temperature, K
t = thickness, m
U_{av} = average velocity in the channels, m/s
W = width of the heat sink, m
w_c = half of the channel width, m
w_w = half of the fin thickness, m
α = thermal diffusivity, m^2/s or constant, $2\xi_u/(1+\alpha_c)$
α_c = channel aspect ratio, $2w_c/H_c$
α_{hs} = heat sink aspect ratio, $L/2w_c$
β = fin spacing ratio, w_c/w_w
γ = ratio of specific heats, c_p/c_v
ΔP = pressure drop across the microchannel/nanochannel, Pa
η_{fin} = efficiency of the fin, $\tanh(mH_c)/mH_c$
λ = mean free path, m
μ = absolute viscosity of fluid, $kg/m \cdot s$
ν = kinematic viscosity of fluid, m^2/s
ξ_u = slip velocity coefficient, $(2-\sigma/\sigma)Kn$
ξ_t = temperature jump coefficient, $(2-\sigma_t/\sigma_t)(2\gamma/\gamma+1)(Kn/Pr)$
ρ = fluid density, kg/m^3
σ = tangential momentum accommodation coefficient
σ_t = energy accommodation coefficient
τ_w = shear stress at channel wall, N/m^2, $\mu\,\frac{du}{dy}|_{y=0}$
ϕ = reduction of the friction factor due to the rarefaction effect, $[(fRe_{Dh})|_{Kn}]/[(fRe_{Dh})|_{Kn=0}]$

Subscripts

a = ambient
av = average
b = base surface
f = fluid
fin = single fin
g = gas
hs = heat sink
s = slip
th = thermal
w = wall

Introduction

CONVENTIONAL heat sinks and heat pipes are unable to handle high heat removal rates. After the pioneering work of Tuckerman and Pease [1], microchannel heat sinks have received considerable attention, especially in microelectronics. Most of these microchannel heat sinks were water cooled. They could dissipate an extremely high-power density with a heat flux as high as 790 W/cm^2 [1]. These heat sinks do not include slip effect.

Received 12 November 2007; revision received 11 February 2008; accepted for publication 12 February 2008.

*Associate Professor, Department of Mechanical Engineering, PN Engineering College.
†Distinguished Professor Emeritus, Department of Mechanical Engineering.

In microchannels/nanochannels, the gas flow can be modeled using Navier–Stokes and energy equations using first-order slip-flow and temperature jump boundary conditions. Microscopic effects become more important when the molecular mean free path of the coolant gas has the same order of magnitude as the channel size. Because of these effects, the friction factors decrease and the heat transfer coefficients increase with increase in Knudsen number.

In this study, the fully developed laminar flow is analyzed through rectangular microchannels/nanochannels in the slip-flow regime ($0.001 < Kn < 0.1$), and closed-form solutions are obtained for friction factors and heat transfer coefficients in terms of the channel aspect ratio, Knudsen number, Reynolds number, and Prandtl number.

There is currently no model for predicting corresponding velocity profiles or pressure distribution in the slip regime. Moreover, there is no such model that can be used in other geometries, for example, two-dimensional channels and rectangular ducts with different aspect ratios. The objective of the current investigation is to develop a unified, physics-based model appropriate for the slip-flow regime and for two-dimensional channels and ducts.

Literature Review

In the last two decades, the flow and heat transfer in microchannel/nanochannel heat sinks have become subjects of growing research attention in microelectronics. Although the work on these channels is not new, microchannel heat sinks have received considerable attention after Tuckerman and Pease [1], especially in microelectronics. Following this work, several experimental, numerical, and theoretical studies on rarefied gas flows in microchannels have been carried out in a wide range of Knudsen numbers with the objective of developing simple, physics-based models. These studies are reviewed in this section.

Harley et al. [2] and, later, Morini et al. [3–5] presented analytical and experimental studies. In these studies, they investigated the rarefaction effects on the pressure drop through silicon microchannels having rectangular, trapezoidal, or double-trapezoidal cross sections. They pointed out the roles of the Knudsen number and the cross-sectional aspect ratio in the friction factor reduction due to the rarefaction and obtained solutions for velocity profiles, friction factors, shear stresses, momentum flux, and kinetic energy correction factors.

Ebert and Sparrow [6] formulated an analytical slip-flow solution for a rectangular channel. They found that the effect of slip is to flatten the velocity distribution relative to that of a continuum flow and that the compressibility increases the pressure drop through an increase in the viscous shear rather than through an increase in the momentum flux.

Inman [7–9] presented theoretical analyses of fluid flow and heat transfer for laminar slip flow in a parallel plate channel with different thermal boundary conditions. The solutions contain a series expansion and analytical expressions for the complete set of eigenvalues and eigenfunctions for the problems. They obtained expressions for the temperature of the gas adjacent to the wall, the wall heat flux, and the Nusselt numbers for the conduits for various values of the rarefaction parameters. The results indicated that the thermal entrance length is decreased with increasing gas rarefaction and also that for a given mean free path the thermal entrance length is greater for unsymmetrical heating than for a symmetrical wall heat flux.

Colin et al. [10] proposed an analytical slip-flow model based on second-order boundary conditions for gaseous flow in rectangular microchannels. They designed an experimental setup for the measurement of gaseous microflow rates under controlled temperature and pressure conditions. It was shown that, in rectangular microchannels, the proposed second-order model is valid for Knudsen numbers up to about 0.25, whereas the first-order model is no longer accurate for values higher than 0.05. The best fit is found for a tangential momentum accommodation coefficient $\sigma = 0.93$, both with helium and nitrogen. Yu and Ameel [11,12] analytically investigated the laminar forced convection in thermally developing slip flow through isoflux rectangular microchannels. They obtained local and fully developed Nusselt numbers, fluid temperatures, and wall temperatures by solving the continuum energy equation for hydrodynamically fully developed slip flow with the velocity slip and temperature jump condition at the walls. They found that the heat transfer may increase, decrease, or remain unchanged, compared with the no-slip flow conditions, depending on the aspect ratios and two-dimensionless variables that include the effects of the microchannel size or rarefaction and the fluid/wall interaction.

Zhao and Lu [13] presented an analytical and numerical study on the heat transfer characteristics of forced convection across a microchannel heat sink. They used porous medium and fin approaches and investigated the effects of channel aspect ratio and effective thermal conductivity ratio on the overall Nusselt number. They found that the overall Nusselt number increases as the channel aspect ratio is increased and decreases with an increasing effective thermal conductivity ratio. They proposed a new concept of microchannel cooling in combination with microheat pipes and estimated the enhancement in the heat transfer. They conducted two-dimensional numerical calculations for both constant heat flux and constant wall temperature conditions to check the accuracy of the analytical solutions and to examine the effect of different boundary conditions on the overall heat transfer.

Quarmby [14] and Gampert [15] used finite-difference simulations to investigate developing slip flow in circular pipes and parallel plates.

Barber and Emerson [16,17] examined the role of Reynolds and Knudsen numbers on the hydrodynamic development length at the entrance to parallel plate microchannels. They carried out numerical simulations over a range of Knudsen numbers covering the continuum and slip-flow regimes. Their results demonstrate that, at the upper limit of the slip-flow regime, the entrance development region is almost 25% longer than that predicted using continuum flow theory.

Andrei and Raymond [18] developed a three-dimensional model to investigate the flow and conjugate heat transfer in the microchannel-based heat sink for electronic packaging applications. They solved the Navier–Stokes equations of motion numerically using the generalized single-equation framework. They also developed and validated the theoretical model by comparing the predictions of the thermal resistance and the friction coefficient with the available experimental data for a wide range of Reynolds numbers. Their analysis provides a unique fundamental insight into the complex heat flow pattern established in the channel due to combined convection–conduction effects in the three-dimensional setting.

Arkilic et al. [19,20] performed analytic and experimental investigations into gaseous flow with slight rarefaction through long microchannels. They used a two-dimensional analysis of the Navier–Stokes equations with a first-order slip-velocity boundary condition to demonstrate that both compressibility and rarefied effects are present in long microchannels. They reported the tangential momentum accommodation coefficients (TMAC) for nitrogen, argon, and carbon dioxide gases in contact with single-crystal silicon. For all three gases, the TMAC is found to be lower than one, ranging from 0.75 to 0.85.

Beskok and Karniadakis [21] developed simple, physics-based models for flows in channels, pipes, and ducts at microscales for a wide range of Knudsen numbers at low Mach numbers. They proposed a new general boundary condition that accounts for the reduced momentum and heat exchange with the wall surfaces and investigated its validity. They found that, as the value of the Knudsen number increases, the rarefaction effects become more important and, thus, the pressure drop, shear stress, heat flux, and corresponding mass flow rate cannot be predicted from standard flow and heat transfer models based on the continuum hypothesis. They also determined that simple models based on kinetic gas theory concepts are not appropriate either, except in the very high Knudsen number regime corresponding to near-vacuum conditions.

Bower et al. [22] presented experimental results on the heat transfer and flow in small SiC heat exchangers with multiple rows of

parallel channels oriented in the flow direction. They analyzed the overall heat transfer and pressure drop coefficients in single-phase flow regimes and found that liquid-cooled SiC heat sinks easily outperform air-cooled heat sinks.

Harms et al. [23] obtained experimental results for a single-phase forced convection in deep rectangular microchannels. They tested single- and multiple-channel systems. All of the tests were performed with deionized water as the working fluid, with the Reynolds number ranging from 173 to 12,900. The experimentally obtained local Nusselt number agreed reasonably well with classical developing channel flow theory. Furthermore, their results show that a multiple-channel system designed for developing laminar flow outperforms the comparable single-channel system designed for turbulent flow.

Hetsroni et al. [24,25] performed experimental and theoretical investigations on single-phase fluid flow and heat transfer in microchannels. They considered both problems in the frame of a continuum model, corresponding to small Knudsen number. They analyzed the data of the pressure drop and heat transfer in circular, triangular, rectangular, and trapezoidal microchannels. The effects of geometry and the axial heat flux due to thermal conduction through the working fluid and channel walls, as well as the energy dissipation, were discussed. They compared the experimental data, obtained by a number of investigators, to the conventional theory on heat transfer.

Hsieh et al. [26,27] presented experimental and theoretical studies of incompressible and compressible flows in a microchannel. They used nitrogen and deionized water as working media in their experiments. The results were found to be in good agreement with those predicted by analytical solutions in which a 2-D continuous flow model with first slip boundary conditions is employed and solved by a perturbation method with a proposed new complete momentum accommodation coefficient.

Analysis

The geometry of a microchannel heat sink is shown in Fig. 1a. The length of the heat sink is L and the width is W. The top surface is insulated, and the bottom surface is uniformly heated. The surfaces of the channels are assumed to be smooth. A coolant passes through a number of microchannels along the x axis and takes heat away from the heat dissipating electronic component attached below. The flow in the channels is steady, laminar, and fully developed. There are N channels, and each channel has a height H_c and width $2w_c$. The thickness of each fin is $2w_w$, whereas the thickness of the base is t_b. The fin tips are assumed to be adiabatic. The temperature of the channel walls is assumed to be T_w with an inlet water temperature of T_a. At the channel wall, the slip-flow velocity and temperature jump boundary conditions were applied to calculate the friction and heat transfer coefficients. Taking advantage of symmetry, a control volume (CV) is selected, as shown in Fig. 1b. The length of the control volume is taken as unity for convenience, and the width and height are taken as $w_w + w_c$ and $H_c + t_b$, respectively. This control volume includes half of the fin and half of the channel along with the base. The side surfaces AB and CD and the top surface AC of this CV can be regarded as impermeable, adiabatic, and shear free (i.e., no mass transfer and shear work transfer across these surfaces). The uniform heat flux over the bottom surface BD of the CV is q.

Governing Equations

The continuum equations for the conservation of mass, momentum, and energy can be used with slip-flow and temperature jump boundary conditions. Using scale analysis, the axial momentum and energy equations for the control volume shown in Fig. 1b reduces to

$$\frac{\mathrm{d}^2u}{\mathrm{d}y^2} = \frac{1}{\mu}\frac{\mathrm{d}p}{\mathrm{d}x} \tag{1}$$

and

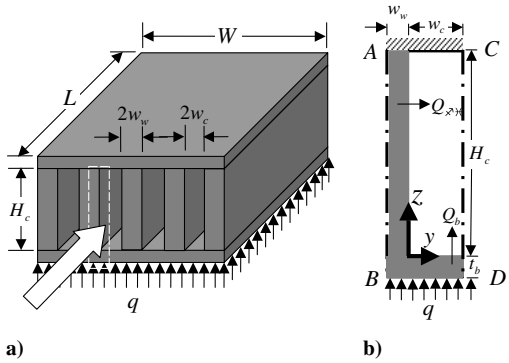

Fig. 1 Geometry of the microchannel/nanochannel heat sink.

$$u\frac{\mathrm{d}T}{\mathrm{d}x} = \alpha\frac{\mathrm{d}^2T}{\mathrm{d}y^2} \tag{2}$$

Hydrodynamic Boundary Conditions

1) At the channel surface:

$$u = u_s = \xi_u\mathcal{L}\frac{\mathrm{d}u}{\mathrm{d}y}\Big|_{y=0}$$

2) At the symmetry plane: $y = w_c\ \frac{\mathrm{d}u}{\mathrm{d}y} = 0$

Thermal Boundary Conditions

1) Following Liu and Garimella [28], the thermal boundary condition at the base of the fin can be determined from an energy balance:

$$-k\frac{\partial T}{\partial y}\bigg|_{y=0} = q\left(\frac{w_w + w_c}{w_w}\right)\left(\frac{2\eta_{\mathrm{fin}}}{2\eta_{\mathrm{fin}} + \alpha_c}\right) = q_w$$

2) At the wall:

$$T_g = T_w - \xi_t\mathcal{L}\frac{\mathrm{d}T}{\mathrm{d}y}\Big|_{y=0}$$

3) At the symmetry plane: $y = w_c\ \frac{\mathrm{d}T}{\mathrm{d}y} = 0$

Fluid Flow

Integrating Eq. (1) twice with respect to y and using hydrodynamic boundary conditions, the velocity distribution in dimensionless form can be written as

$$u(\eta) = -Aw_c^2(2\eta - \eta^2 + 4\alpha) \tag{3}$$

The average velocity in the channel is defined as

$$U_{\mathrm{av}} = \frac{1}{w_c}\int_0^{w_c} u(y)\,\mathrm{d}y = -\frac{2}{3}Aw_c(1 + 6\alpha) \tag{4}$$

The normalized velocity distribution and slip-flow velocity can be written as

$$\left.\begin{array}{c} \frac{u(\eta)}{U_{\mathrm{av}}} = \frac{3}{2}\left(\frac{2\eta-\eta^2+4\alpha}{1+6\alpha}\right) \\ \frac{U_s}{U_{\mathrm{av}}} = \frac{6\alpha}{1+6\alpha} \end{array}\right\} \tag{5}$$

The momentum transfer to the channel wall can be expressed in terms of the skin-friction coefficient or friction factor, defined as

$$f = \frac{\tau_w}{\frac{1}{2}\rho U_{\mathrm{av}}^2} = \frac{24}{Re_{D_h}}\cdot\frac{1}{1+\alpha_c}\cdot\frac{1}{1+6\alpha} \tag{6}$$

which gives the Poiseuille number fRe_{D_h} for rectangular microchannels/nanochannels in terms of aspect ratio α_c and the slip-velocity coefficient.

$$fRe_{D_h} = [24/(1+\alpha_c)] \cdot [1/(1+6\alpha)] \tag{7}$$

The values of the Poiseuille number are compared with the analytical values quoted by Shah and London [29] and the numerical values given by Morini et al. [4] in Table 1 for the continuum flow (Kn = 0). Morini et al. [4] defined the reduction of the friction factor due to the rarefaction effect as follows:

$$\phi = \frac{(fRe_{Dh})\Big|_{Kn}}{(fRe_{Dh})\Big|_{Kn=0}} = \frac{1}{1+\frac{12}{1+\alpha_c}\left(\frac{2-\sigma}{\sigma}\right)Kn} \tag{8}$$

For a fixed cross section, the friction factor reduction ϕ has been calculated by comparing the Poiseuille number for an assigned value of the Knudsen number with the value that the Poiseuille number assumes for $Kn = 0$ (i.e., the continuum flow). The friction factor reduction ϕ depends on the channel aspect ratio and on the Knudsen number.

Table 2 shows the comparison of the present values of the friction factor reduction ϕ with the numerical values presented by Morini et al. [4] for some values of the Knudsen number between 0.001 and 0.1. It shows that ϕ decreases as Kn goes from 0.001 to 0.1; this result confirms that gas rarefaction reduces the friction between the gas and the microchannel/nanochannel walls. The reduction of the friction factor is stronger for rectangular microchannels/nanochannels with small channel aspect ratios. For $Kn = 0$, the friction factor reduction ϕ reaches the minimum value of 45.5; the value of ϕ becomes 56.5% for a square microchannel/nanochannel ($\alpha_c = 1$).

The rectangular microchannels/nanochannels with smaller channel aspect ratios have higher values of α_c; hence, for these microchannels/nanochannels, the decrease of the friction factor with the Knudsen number is larger. In other words, the rarefaction effects appear to be higher in microchannels/nanochannels with smaller aspect ratios. This is due to the definition of the Knudsen number based on the hydraulic diameter of the channel.

It shows that the present values are in good agreement for smaller aspect ratios with the previous results. This can be considered a good validation of the assumptions made in the present work.

The coefficient of pressure loss can be determined from

$$K = \Delta P / \left(\tfrac{1}{2}\rho U_{\text{av}}^2\right) = k_{\text{ce}} + f(L/D_h) \tag{9}$$

where k_{ce} is the sum of the contraction and expansion losses in the channel. Kleiner et al. [30] used experimental data from Kays and London [31] and derived the following empirical correlation for the entrance and exit losses k_{ce} in terms of the channel width and fin thickness:

$$k_{\text{ce}} = 1.79 - 2.32[w_c/(w_c+w_w)] + 0.53[w_c/(w_c+w_w)]^2 \tag{10}$$

Table 1 Comparison of Poiseuille numbers fRe_{D_h} for microchannels/nanochannels

	Poiseuille number fRe_{D_h}		
α_c	Shah and London [29]	Morini et al. [4]	Present
0	24	24	24
0.2	19.07	19.07	20.00
0.4	16.37	16.37	17.14
0.6	14.98	14.98	15.00
0.8	14.37	14.37	13.33
1.0	14.22	14.22	12.00

Heat Transfer

The energy equation, Eq. (2), in dimensionless form can be written as

$$(1+2\alpha_c)f(\eta)\frac{\partial\Theta}{\partial\xi} = \frac{4}{Pe_{D_h}}\frac{\partial^2\Theta}{\partial\eta^2} \tag{11}$$

where

$$\xi = x/w_c, \qquad \eta = y/w_c, \qquad f(\eta) = \frac{3}{2}\left(\frac{2\eta-\eta^2+4\alpha}{1+6\alpha}\right)$$

$$\Theta = \frac{T-T_a}{D_h q_w/k_f}, \qquad U_{\text{av}} = u/f(\eta), \qquad Pe_{D_h} = Re_{D_h}Pr$$

From an energy balance on a fluid element in the channel,

$$\frac{\mathrm{d}T}{\mathrm{d}x} = \frac{\alpha(q_w/k_f)}{w_c U_{\text{av}}} \tag{12}$$

In dimensionless form, it can be written as

$$\partial\Theta/\partial\xi = 1/Pe_{D_h} \tag{13}$$

Combining Eqs. (11) and (13), we get

$$\frac{\partial^2\Theta}{\partial\eta^2} = \frac{1+\alpha_c}{4}f(\eta) = \left(\frac{1+\alpha_c}{4}\right)\left[\left(3\eta-\frac{3}{2}\eta^2\right) + \left(1-3\eta+\frac{3}{2}\eta^2\right)\frac{U_s}{U_{\text{av}}}\right] \tag{14}$$

In dimensionless form, first thermal boundary condition can be written as

Table 2 Comparison of friction factor reduction (ϕ) for microchannels/nanochannels

	Friction factor reduction (ϕ)					
	$Kn = 0.001$		$Kn = 0.01$		$Kn = 0.1$	
α_c	Present	Morini et al. [4]	Present	Morini et al. [4]	Present	Morini et al. [4]
0.0	0.988	0.988	0.893	0.893	0.455	0.455
0.1	0.989	0.989	0.902	0.901	0.478	0.477
0.2	0.990	0.990	0.909	0.907	0.500	0.496
0.3	0.991	0.990	0.916	0.912	0.520	0.514
0.4	0.991	0.991	0.921	0.917	0.539	0.529
0.5	0.992	0.991	0.926	0.920	0.556	0.541
0.6	0.992	0.992	0.930	0.923	0.571	0.551
0.7	0.993	0.992	0.934	0.924	0.586	0.557
0.8	0.993	0.992	0.937	0.925	0.600	0.562
0.9	0.994	0.992	0.941	0.925	0.613	0.564
1.0	0.994	0.992	0.943	0.926	0.625	0.565

$$-k\left.\frac{\partial\Theta_s}{\partial\eta}\right|_{\eta=0}=\frac{k_f w_c}{D_h} \tag{15}$$

where

$$\Theta_s=\frac{T-T_w}{D_h q_w/k_f}$$

is the dimensionless temperature for the solid surface. Also, from the continuity of the temperature and heat flux at the solid–fluid interface,

$$-k\left.\frac{\partial\Theta_s}{\partial\eta}\right|_{\eta=0}=-k_f\left.\frac{\partial\Theta}{\partial\eta}\right|_{\eta=0} \tag{16}$$

Combining Eqs. (15) and (16), we get

$$\left.\frac{\partial\Theta}{\partial\eta}\right|_{\eta=0}=-\frac{w_c}{D_h} \tag{17}$$

Using this boundary condition and integrating Eq. (14) with respect to η, we get

$$\frac{\partial\Theta}{\partial\eta}=\left(\frac{1+\alpha_c}{4}\right)\left[\left(\frac{3}{2}\eta^2-\frac{1}{2}\eta^3-1\right)+\left(\eta-\frac{3}{2}\eta^2+\frac{1}{2}\eta^3\right)\frac{U_s}{U_{\text{av}}}\right] \tag{18}$$

From an overall energy balance on the fluid element, we get the following additional condition

$$\int_0^1 f(\eta)\cdot\Theta(\eta)\,\mathrm{d}\eta=0 \tag{19}$$

Integrating Eq. (18) and applying Eq. (19), we get

$$\Theta(\eta)=(1+\alpha_c)\left[\left(\frac{1}{8}\eta^3-\frac{1}{32}\eta^4-\frac{1}{4}\eta+\frac{17}{140}\right)+\frac{1}{210}\left(\frac{U_s}{U_{\text{av}}}\right)^2+\left(\frac{1}{8}\eta^2-\frac{1}{8}\eta^3-\frac{1}{32}\eta^4-\frac{3}{70}\right)\frac{U_s}{U_{\text{av}}}\right] \tag{20}$$

Integrating Eq. (13) and applying the condition

$$\Theta=\frac{T_g-T_a}{D_h q_w/k_f}$$

at $\eta=0$, we get

$$\frac{T_g-T_a}{D_h q_w/k_f}=\frac{\xi}{Pe_{D_h}}+\Theta(0) \tag{21}$$

where $\Theta(0)$ can be determined from Eq. (18). From the second thermal boundary condition, we get

$$\frac{T_g-T_w}{D_h q_w/k_f}=\xi_t \tag{22}$$

Combining Eqs. (21) and (22), we get

$$\frac{T_w-T_a}{D_h q_w/k_f}=\frac{\xi}{Pe_{D_h}}+\Theta(0)+\xi_t \tag{23}$$

By definition, the bulk temperature is given by

$$T_b=T_a+\frac{(D_h q_w/k_f)\xi}{Pe_{D_h}} \tag{24}$$

which gives

$$\frac{T_b-T_a}{D_h q_w/k_f}=\frac{\xi}{Pe_{D_h}} \tag{25}$$

Combining Eqs. (23) and (25), we get

$$\frac{T_w-T_b}{D_h q_w/k_f}=\Theta(0)+\xi_t=(1+\alpha_c)\left[\frac{17}{140}-\frac{3}{70}\frac{U_s}{U_{\text{av}}}+\frac{1}{210}\left(\frac{U_s}{U_{\text{av}}}\right)^2\right]+\xi_t \tag{26}$$

For uniform wall flux (UWF), the average heat transfer coefficient for the fin is defined as

$$h_{\text{fin}}=q_w/(T_w-T_b) \tag{27}$$

In dimensionless form it can be written as

$$Nu_{D_h}=\frac{h_{\text{fin}}D_h}{k_f} \tag{28}$$

Overall Heat Transfer Coefficient for the Heat Sink

The heat balance for the whole CV can be written as

$$Q=NQ_{\text{fin}}+Q_b \tag{29}$$

where

$$\left.\begin{array}{c}Q=(h\eta A)_{\text{hs}}\theta_b\\ Q_{\text{fin}}=(hA\eta)_{\text{fin}}\theta_b\\ Q_b=(hA)_b\theta_b\end{array}\right\} \tag{30}$$

which gives the overall average heat transfer coefficient for a microchannel/nanochannel heat sink:

$$h_{\text{hs}}=\frac{(N+1)(Ah\eta)_{\text{fin}}+(hA)_b}{(\eta A)_{\text{hs}}} \tag{31}$$

with

$$\left.\begin{array}{c}N=(W-2w_w)/2(w_c+w_w)\\ A_{\text{hs}}=NA_{\text{fin}}+A_b\\ \eta_{\text{hs}}=1-(NA_{\text{fin}}/A_{\text{hs}})(1-\eta_{\text{fin}})\\ A_{\text{fin}}=2H_c(2w_w+L)\\ A_b=LW-(N+1)(2w_wL)\end{array}\right\} \tag{32}$$

The average heat transfer coefficient for the fin can be determined from Eq. (29), whereas h_b for the UWF boundary condition was determined by Khan et al. [32] and could be written as

$$h_b=0.912(k_f/L)Re_L^{1/2}Pr^{1/3} \tag{33}$$

where Re_L is the Reynolds number based on the length of the base plate and is defined as

$$Re_L=(U_{\text{av}}L)/\nu \tag{34}$$

Case Studies and Discussion

The slip-flow range ($0.001<Kn<0.1$) dictates the channel width for the flow of any gas through microchannels/nanochannels. For air ($\lambda=69.2$ nm), Fig. 2 shows that the channel width ranges from 35 μm to 350 nm. Qin and Li [33] have shown a novel technique in creating microchannels/nanochannels using a Nd:YAG laser in a dry process.

In these channels, the friction losses are reduced, as shown in Fig. 3. It is demonstrated that the friction losses are highest in the continuum flow ($Kn=0$). As the Kn number increases, the friction losses decrease with an increase in the aspect ratio. Arkilic et al. [19,20] demonstrated experimentally that, for nitrogen, argon, and carbon dioxide, the TMAC is found to be lower than 1, ranging from 0.75 to 0.85. The effect of these TMAC on the friction factors are shown in Fig. 4 in the slip region. It shows that the friction factors decrease monotonically as TMAC decreases and the channel aspect ratio increases. The effects of the aspect ratios on the pressure drop in the slip-flow region are investigated in Fig. 5. It is obvious that the

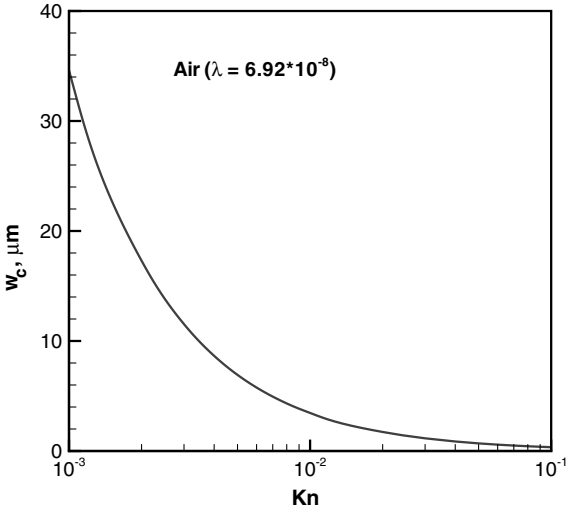

Fig. 2 Channel width in the slip-flow region.

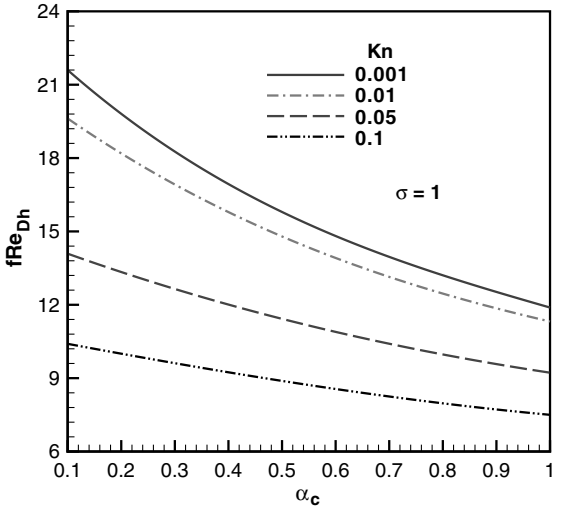

Fig. 3 Effect of channel aspect ratios on friction factors in the slip-flow region.

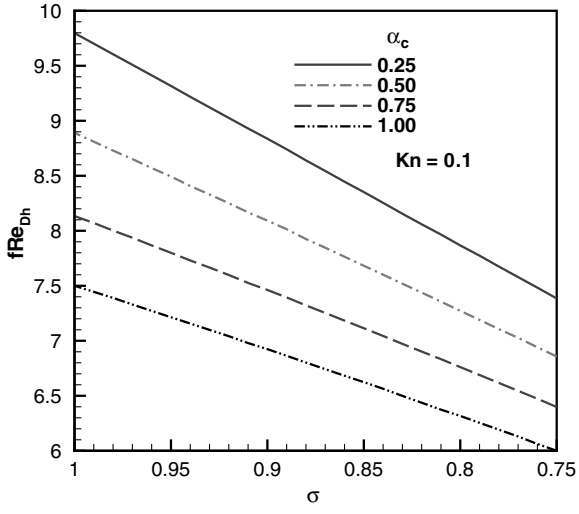

Fig. 4 Effect of tangential momentum accommodation coefficient on friction factors.

pressure drop is higher for lower aspect ratios. The pressure drop in microchannels/nanochannels decreases with an increase in the aspect ratios. The dimensionless heat transfer coefficient decreases with an increase in the Knudsen numbers and aspect ratios as well. This trend is shown in Fig. 6. The effect of the Kn number is to decrease the value of the Nusselt number below its continuum value, and this reduction increases significantly with an increasing Kn number. Figure 7 shows the effect of the volume flow rate on the average heat transfer from a microchannel/nanochannel heat sink. It is obvious that the average heat transfer increases with the increase in the volume flow rate and aspect ratio.

Conclusions

The continuum momentum and energy equations are solved for laminar forced convection in two-dimensional rectangular microchannels and nanochannels under hydrodynamically and thermally fully developed conditions with the first-order velocity slip and temperature jump boundary conditions at the channel walls. Closed-form solutions are obtained for the fluid friction and Nusselt numbers in the slip-flow regime. It is demonstrated that the friction losses decrease with the decrease in Knudsen numbers and the increase in the channel aspect ratios, whereas the dimensionless heat transfer

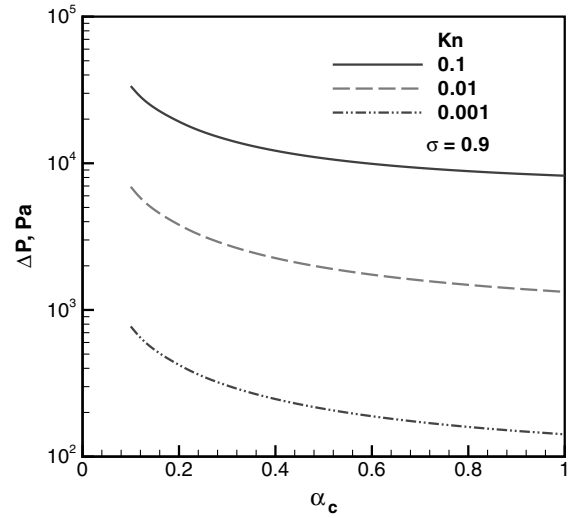

Fig. 5 Effect of the Knudsen number on the pressure drop.

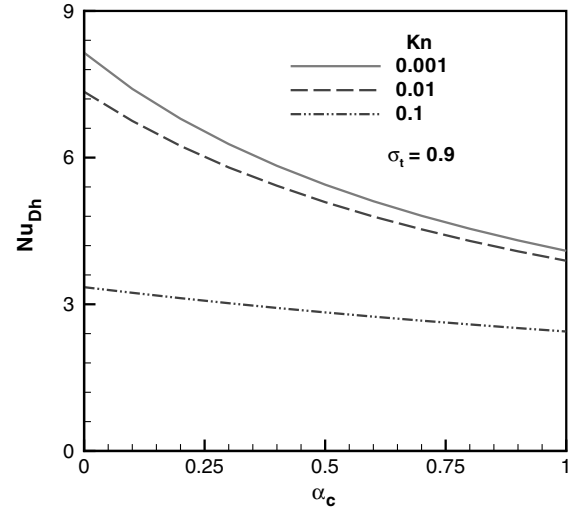

Fig. 6 Effect of α_c on the heat transfer from the fin in the slip-flow region.

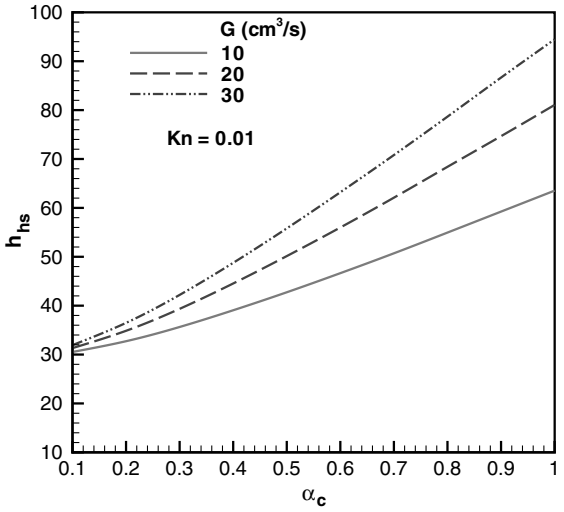

Fig. 7 Effect of the volume flow rate on the average heat transfer from the microchannel/nanochannel heat sink.

coefficient for the channel decreases with the increase in Knudsen numbers and aspect ratios as well.

Acknowledgments

The authors gratefully acknowledge the financial support of the Natural Sciences and Engineering Research Council of Canada and the Center for Microelectronics Assembly and Packaging.

References

[1] Tuckerman, D. B., and Pease, R. F. W., "High-Performance Heat Sinking for VLSI," *IEEE Electron Device Letters*, Vol. 2, No. 5, May 1981, pp. 126–129. doi:10.1109/EDL.1981.25367

[2] Harley, J. C., Huang, Y., Bau, H. H., and Zewel, J. N., "Gas Flow in Micro-Channels," *Journal of Fluid Mechanics*, Vol. 284, 1995, pp. 257–274. doi:10.1017/S0022112095000358

[3] Morini, G. L., and Spiga, M., "Slip Flow in Rectangular Microtubes," *Microscale Thermophysical Engineering*, Vol. 2, No. 4, 1998, pp. 273–282. doi:10.1080/108939598199919

[4] Morini, G. L., Spiga, M., and Tartarini, P., "The Rarefaction Effect on the Friction Factor of Gas Flow in Micro/Nano-Channels," *Superlattices and Microstructures*, Vol. 35, Nos. 3–6, 2004, pp. 587–599. doi:10.1016/j.spmi.2003.09.013

[5] Morini, G. L., Lorenzini, M., and Spiga, M., "A Criterion for Experimental Validation of Slip-Flow Models for Incompressible Rarefied Gases Through Micro/Nano-Channels," *Microfluidics and Nanofluidics*, Vol. 1, No. 2, 2005, pp. 190–196. doi:10.1007/s10404-004-0028-1

[6] Ebert, W. A., and Sparrow, E. M., "Slip Flow in Rectangular and Annular Ducts," *Journal of Basic Engineering*, Vol. 87, 1965, pp. 1018–1024.

[7] Inman, R. M., "Heat Transfer for Laminar Slip Flow of a Rarefied Gas in a Parallel Plate Channel or a Round Tube with Uniform Wall Heating," NASA TN D-2393, Aug. 1964.

[8] Inman, R. M., "Heat Transfer for Laminar Slip Flow of a Rarefied Gas in a Parallel Plate Channel or a Circular Tube with Uniform Wall Temperature," NASA TN D-2213, Nov. 1964.

[9] Inman, R. M., "Heat Transfer for Laminar Slip Flow of a Rarefied Gas Between Parallel Plates with Unsymmetrical Wall Heat Flux," NASA TN D-2421, Aug. 1964.

[10] Colin, S., Lalonde, P., and Caen, R., "Validation of a Second-Order Slip Flow Model in Rectangular Microchannels," *Heat Transfer Engineering*, Vol. 25, No. 3, 2004, pp. 23–30. doi:10.1080/01457630490280047

[11] Yu, S., and Ameel, T. A., "Slip Flow Heat Transfer in Rectangular Microchannels," *International Journal of Heat and Mass Transfer*, Vol. 44, No. 22, 2001, pp. 4225–4234. doi:10.1016/S0017-9310(01)00075-8

[12] Yu, S., and Ameel, T. A., "Slip Flow Convection in Isoflux Rectangular Microchannels," *Journal of Heat Transfer*, Vol. 124, No. 2, April 2002, pp. 346–355. doi:10.1115/1.1447932

[13] Zhao, C. Y., and Lu, T. J., "Analysis of Microchannel Heat Sinks for Electronics Cooling," *International Journal of Heat and Mass Transfer*, Vol. 45, No. 24, Nov. 2002, pp. 4857–4869. doi:10.1016/S0017-9310(02)00180-1

[14] Quarmby, A., "A Finite-Difference Analysis of Developing Slip Flow," *Applied Scientific Research*, Vol. 19, No. 1, Jan. 1968, pp. 18–33. doi:10.1007/BF00383909

[15] Gampert, B., "Inlet Flow With Slip," *Rarefied Gas Dynamics*, Vol. 10, 1976, pp. 225–235.

[16] Barber, R. W., and Emerson, D. R., "A Numerical Investigation of Low Reynolds Number Gaseous Slip Flow at the Entrance of Circular and Parallel Plate Micro-Channels," *ECCOMAS Computational Fluid Dynamics Conference 2001*, Sept. 2001.

[17] Barber, R. W., and Emerson, D. R., "The Influence of Knudsen Number on the Hydrodynamic Development Length Within Parallel Plate Micro-Channels," *Advances in Fluid Mechanics IV*, edited by M. Rahman, R. Verhoeven, and C. A. Brebbia, WIT Press, Southampton, England, U.K., 2002, pp. 207–216.

[18] Andrei, G. F., and Raymond, V., "Three-Dimensional Conjugate Heat Transfer in the Micro-Channel Heat Sink for Electronic Packaging," *International Journal of Heat and Mass Transfer*, Vol. 43, No. 3, 2000, pp. 399–415. doi:10.1016/S0017-9310(99)00151-9

[19] Arkilic, E. B., Breuer, K. S., and Schmidt, M. A., "Mass Flow and Tangential Momentum Accommodation in Silicon Micromachined Channels," *Journal of Fluid Mechanics*, Vol. 437, 2001, pp. 29–43. doi:10.1017/S0022112001004128

[20] Arkilic, E. B., Schmidt, M. A., and Breuer, K. S., "Gaseous Slip Flow in Long Microchannels," *Journal of Microelectromechanical Systems*, Vol. 6, No. 2, 1997, pp. 167–178. doi:10.1109/84.585795

[21] Beskok, A., and Karniadakis, G. E., "A Model for Flows in Channels, Pipes, and Ducts at Micro Scales," *Microscale Thermophysical Engineering*, Vol. 3, No. 1, Feb. 1999, pp. 43–77. doi:10.1080/108939599199864

[22] Bower, C., Ortega, A., Skandakumaran, P., Vaidyanathan, R., Green, C., and Phillips, T., "Heat Transfer in Water-Cooled Silicon Carbide Milli-Channel Heat Sinks for High Power Electronic Applications," *2003 ASME International Mechanical Engineering Congress & Exposition*, American Society of Mechanical Engineers, New York, Nov. 2003, pp. 327–335.

[23] Harms, T. M., Kazmierczak, M. J., and Gerner, F. M., "Developing Convective Heat Transfer in Deep Rectangular Microchannels," *International Journal of Heat and Fluid Flow*, Vol. 20, No. 2, April 1999, pp. 149–157. doi:10.1016/S0142-727X(98)10055-3

[24] Hetsroni, G., Mosyak, A., Pogrebnyak, E., and Yarin, L. P., "Fluid Flow in Micro-Channels," *International Journal of Heat and Mass Transfer*, Vol. 48, No. 10, May 2005, pp. 1982–1998. doi:10.1016/j.ijheatmasstransfer.2004.12.019

[25] Hetsroni, G., Mosyak, A., Pogrebnyak, E., and Yarin, L. P., "Heat Transfer in Micro-Channels: Comparison of Experiments with Theory and Numerical Results," *International Journal of Heat and Mass Transfer*, Vol. 48, Nos. 25–26, Dec. 2005, pp. 5580–5601. doi:10.1016/j.ijheatmasstransfer.2005.05.041

[26] Hsieh, S. S., Tsai, H. H., Lin, C. Y., Huang, C. F., and Chien, C. M., "Gas Flow in a Long Microchannel," *International Journal of Heat and Mass Transfer*, Vol. 47, Nos. 17–18, Aug. 2004, pp. 3877–3887. doi:10.1016/j.ijheatmasstransfer.2004.03.027

[27] Hsieh, S. S., Lin, C. Y., Huang, C. F., and Tsai, H. H., "Liquid Flow in a Micro-Channel," *Journal of Micromechanics and Microengineering*, Vol. 14, No. 4, April 2004, pp. 436–445. doi:10.1088/0960-1317/14/4/002

[28] Liu, D., and Garimella, S. V., "Analysis and Optimization of the Thermal Performance of Microchannel Heat Sinks", *International Journal for Numerical Methods in Heat & Fluid Flow*, Vol. 15, No. 1, 2005, pp. 7–26.

[29] Shah, R. K., and London, A. L., "Laminar Flow Forced Convection in Ducts," *Advances in Heat Transfer*, Vol. 14, Supplement 1, 1978, p. 196.

[30] Kleiner, M. B., Kuhn, S. A., and Haberger, K., "High Performance Forced Air Cooling Scheme Employing Microchannel Heat Exchangers," *IEEE Transactions on Components, Packaging, and Manufacturing Technology. Part A*, Vol. 18, No. 4, 1995, pp. 795–804. doi:10.1109/95.477466

[31] Kays, W. M., and London, A. L., *Compact Heat Exchangers*, McGraw–Hill, New York, 1964.

[32] Khan, W. A., Culham, J. R., and Yovanovich, M. M., "Fluid Flow Around and Heat Transfer from Elliptical Cylinders: Analytical Approach," *Journal of Thermophysics and Heat Transfer*, Vol. 19, No. 2, 2005, pp. 178–185.

[33] Qin, J. S. J., and Li, W. J., "Fabrication of Complex Micro Channel Systems Inside Optically-Transparent 3D Substrates by Laser Processing," *11th International Conference on Solid-State Sensors and Actuators*, Springer–Verlag, Berlin, June 2001, pp. 1624–1627.